

ON INCREASING OF DENSITY OF HETEROTRANSISTORS IN THE FRAMEWORK OF A CMOS OPERATIONAL TRANSRESISTANCE AMPLIFIER

E.L. Pankratov

Nizhny Novgorod State University, 23 Gagarin avenue, Nizhny Novgorod,
603950, Russia

Nizhny Novgorod State Agrotechnical University, 97 Gagarin avenue, Nizhny Novgo-
rod, 603950, Russia

ABSTRACT

We introduce an approach for increasing of density of field-effect heterotransistors in the framework of a CMOS operational transresistance amplifier based square wave generator. Based on the approach we consider manufacturing the considered amplifier in a heterostructure with the required configuration. Several required areas of the heterostructure should be doped by diffusion or ion implantation. After that dopant and radiation defects should be annealed in the framework of an optimized scheme. We also consider an approach to decrease value of mismatch-induced stress in the considered heterostructure. We introduce an analytical approach to analyze mass and heat transport in heterostructures during manufacturing of integrated circuits with account mismatch-induced stress.

KEYWORDS

CMOS operational transresistance amplifier; optimization of manufacturing; analytical approach for prognosis.

1. INTRODUCTION

Currently some problems of the electronics of the solid state solving with high rate [1-6]. To increase performance of electronics of the solid state devices it is necessary to determine materials with larger mobility of carriers of charge [7-10]. One way to decrease dimensions of elements of integrated circuits is manufacturing them in thin film heterostructures [3-5,11]. In this case it is possible to use inhomogeneity of heterostructure and necessary optimization of doping of electronic materials [12] and development of epitaxial technology to improve these materials (including analysis of mismatch induced stress) [13-15]. An alternative approaches to increase dimensions of integrated circuits are using of laser and microwave types of annealing [16,17].

We consider a method of optimization of manufacturing of transistors in a CMOS operational transresistance amplifier [18]. The optimization leads to increase integration rate of transistors. The approach gives a possibility to decrease their dimensions with increasing their density. We also consider possibility to decrease mismatch-induced stress to decrease quantity of defects, generated due to the stress. In this paper we consider a heterostructure, which consist of a substrate and an epitaxial layer (see Fig. 1b). We consider the third layer in the heterostructure: buffer layer between epitaxial layer and substrate (the buffer layer is usually help to decrease mis-

match-induced stress). The epitaxial layer includes into itself several sections, which were manufactured by using another materials. These sections have been doped by diffusion or ion implantation to manufacture the required types of conductivity (p or n). These areas became sources, drains and gates in field-effect transistors in the framework of the CMOS operational transresistance amplifier. Circuit of the amplifier is presented on the Fig. 1a. After this doping it is required annealing of dopant and/or radiation defects. Main aim of the present paper is analysis of redistribution of dopant and radiation defects to determine conditions, which correspond to decreasing of elements of the considered amplifier and at the same time to increase their density. We present a method for decreasing mismatch-induced stress.

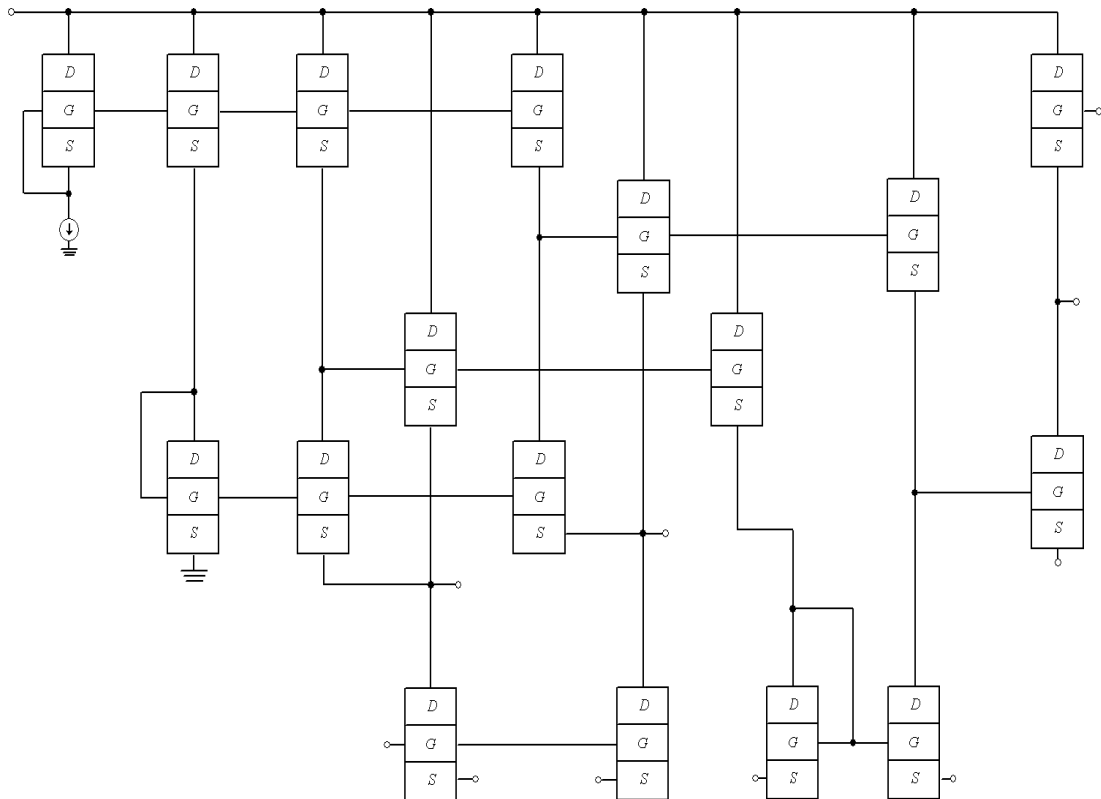


Fig. 1a. Structure of considered amplifier [18]

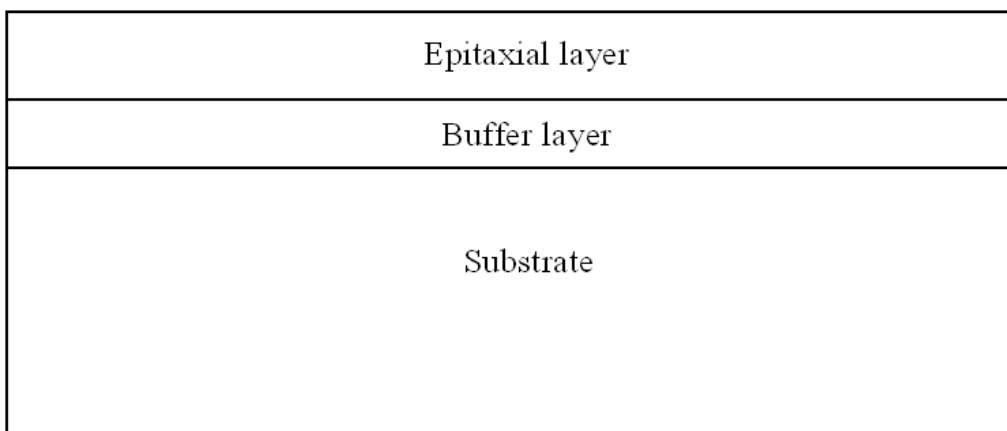


Fig. 1b. Heterostructure with a substrate, epitaxial layers and buffer layer (view from side)

2. METHOD OF SOLUTION

To solve our aim we determine and analyzed spatio-temporal distribution of concentration of dopant in the considered heterostructure. We determine the distribution by solving the second Fick's law in the following form [1,19-22]

$$\begin{aligned} \frac{\partial C(x, y, z, t)}{\partial t} = & \frac{\partial}{\partial x} \left[D \frac{\partial C(x, y, z, t)}{\partial x} \right] + \frac{\partial}{\partial y} \left[D \frac{\partial C(x, y, z, t)}{\partial y} \right] + \frac{\partial}{\partial z} \left[D \frac{\partial C(x, y, z, t)}{\partial z} \right] + \\ & + \Omega \frac{\partial}{\partial x} \left[\frac{D_s}{kT} \nabla_s \mu_1(x, y, z, t) \int_0^{L_z} C(x, y, W, t) dW \right] + \\ & + \Omega \frac{\partial}{\partial y} \left[\frac{D_s}{kT} \nabla_s \mu_1(x, y, z, t) \int_0^{L_z} C(x, y, W, t) dW \right] + (1) \\ & + \frac{\partial}{\partial x} \left[\frac{D_{cs}}{\bar{V} kT} \frac{\partial \mu_2(x, y, z, t)}{\partial x} \right] + \frac{\partial}{\partial y} \left[\frac{D_{cs}}{\bar{V} kT} \frac{\partial \mu_2(x, y, z, t)}{\partial y} \right] + \frac{\partial}{\partial z} \left[\frac{D_{cs}}{\bar{V} kT} \frac{\partial \mu_2(x, y, z, t)}{\partial z} \right]. \end{aligned}$$

Initial and boundary conditions for the above equation could be written as

$$\begin{aligned} \left. \frac{\partial C(x, y, z, t)}{\partial x} \right|_{x=0} = 0, \quad \left. \frac{\partial C(x, y, z, t)}{\partial x} \right|_{x=L_x} = 0, \quad \left. \frac{\partial C(x, y, z, t)}{\partial y} \right|_{y=0} = 0, \quad C(x, y, z, 0) = f_C(x, y, z), \\ \left. \frac{\partial C(x, y, z, t)}{\partial y} \right|_{x=L_y} = 0, \quad \left. \frac{\partial C(x, y, z, t)}{\partial z} \right|_{z=0} = 0, \quad \left. \frac{\partial C(x, y, z, t)}{\partial z} \right|_{x=L_z} = 0. \end{aligned}$$

Here $C(x, y, z, t)$ is the spatio-temporal distribution of concentration of dopant; Ω is the atomic vo

lume of dopant; ∇_s is the symbol of surficial gradient; $\int_0^{L_z} C(x, y, z, t) d z$ is the dopant's concen

tration on heterostructure's interface, which is perpendicular to Z-axis; D and D_s are the coefficients of volumetric and surficial diffusions; functions $\mu_1(x, y, z, t)$ and $\mu_2(x, y, z, t)$ describe the chemical potentials: $\mu_1(x, y, z, t)$ corresponds to mismatch-induced stress in the considered heterostructure, $\mu_2(x, y, z, t)$ corresponds to porosity of materials of the considered heterostructure. Values of dopant diffusions coefficients depends on properties of materials of heterostructure, speed of heating and cooling of materials during annealing and spatio-temporal distribution of concentration of dopant. Dependences of dopant diffusions coefficients on parameters could be approximated by the following relations [23-25]

$$D_C = D_L(x, y, z, T) \left[1 + \xi \frac{C^\gamma(x, y, z, t)}{P^\gamma(x, y, z, T)} \right] \left[1 + \varsigma_1 \frac{V(x, y, z, t)}{V^*} + \varsigma_2 \frac{V^2(x, y, z, t)}{(V^*)^2} \right],$$

$$D_S = D_{SL}(x, y, z, T) \left[1 + \xi_S \frac{C^\gamma(x, y, z, t)}{P^\gamma(x, y, z, T)} \right] \left[1 + \zeta_1 \frac{V(x, y, z, t)}{V^*} + \zeta_2 \frac{V^2(x, y, z, t)}{(V^*)^2} \right]. \quad (2)$$

Here $D_L(x, y, z, T)$ and $D_{LS}(x, y, z, T)$ are the spatial (due to accounting all layers of heterostructure) and temperature (due to Arrhenius law) dependences of dopant diffusion coefficients; T is the temperature of annealing; $P(x, y, z, T)$ is the limit of solubility of dopant; parameter γ depends on properties of materials and could be integer in the following interval $\gamma \in [1, 3]$ [23]; $V(x, y, z, t)$ is the spatio-temporal distribution of concentration of radiation vacancies; V^* is the equilibrium distribution of vacancies. Concentrational dependence of dopant diffusion coefficient has been described in details in [23]. Spatio-temporal distributions of concentration of point radiation defects have been determined by solving the following system of equations [19-22, 24, 25]

$$\begin{aligned} \frac{\partial I(x, y, z, t)}{\partial t} = & \frac{\partial}{\partial x} \left[D_I(x, y, z, T) \frac{\partial I(x, y, z, t)}{\partial x} \right] + \frac{\partial}{\partial y} \left[D_I(x, y, z, T) \frac{\partial I(x, y, z, t)}{\partial y} \right] + \\ & + \frac{\partial}{\partial z} \left[D_I(x, y, z, T) \frac{\partial I(x, y, z, t)}{\partial z} \right] - k_{I,I}(x, y, z, T) I^2(x, y, z, t) - k_{I,V}(x, y, z, T) \times \\ & \times I(x, y, z, t) V(x, y, z, t) + \Omega \frac{\partial}{\partial x} \left[\frac{D_{IS}}{kT} \nabla_s \mu(x, y, z, t) \int_0^{L_z} I(x, y, W, t) dW \right] + \\ & + \Omega \frac{\partial}{\partial y} \left[\frac{D_{IS}}{kT} \nabla_s \mu(x, y, z, t) \int_0^{L_z} I(x, y, W, t) dW \right] + \frac{\partial}{\partial x} \left[\frac{D_{IS}}{\bar{V} kT} \frac{\partial \mu_2(x, y, z, t)}{\partial x} \right] + \\ & + \frac{\partial}{\partial y} \left[\frac{D_{IS}}{\bar{V} kT} \frac{\partial \mu_2(x, y, z, t)}{\partial y} \right] + \frac{\partial}{\partial z} \left[\frac{D_{IS}}{\bar{V} kT} \frac{\partial \mu_2(x, y, z, t)}{\partial z} \right] \end{aligned} \quad (3)$$

$$\begin{aligned} \frac{\partial V(x, y, z, t)}{\partial t} = & \frac{\partial}{\partial x} \left[D_V(x, y, z, T) \frac{\partial V(x, y, z, t)}{\partial x} \right] + \frac{\partial}{\partial y} \left[D_V(x, y, z, T) \frac{\partial V(x, y, z, t)}{\partial y} \right] + \\ & + \frac{\partial}{\partial z} \left[D_V(x, y, z, T) \frac{\partial V(x, y, z, t)}{\partial z} \right] - k_{V,V}(x, y, z, T) V^2(x, y, z, t) - k_{I,V}(x, y, z, T) \times \\ & \times I(x, y, z, t) V(x, y, z, t) + \Omega \frac{\partial}{\partial x} \left[\frac{D_{VS}}{kT} \nabla_s \mu(x, y, z, t) \int_0^{L_z} V(x, y, W, t) dW \right] + \\ & + \Omega \frac{\partial}{\partial y} \left[\frac{D_{VS}}{kT} \nabla_s \mu(x, y, z, t) \int_0^{L_z} V(x, y, W, t) dW \right] + \frac{\partial}{\partial x} \left[\frac{D_{VS}}{\bar{V} kT} \frac{\partial \mu_2(x, y, z, t)}{\partial x} \right] + \\ & + \frac{\partial}{\partial y} \left[\frac{D_{VS}}{\bar{V} kT} \frac{\partial \mu_2(x, y, z, t)}{\partial y} \right] + \frac{\partial}{\partial z} \left[\frac{D_{VS}}{\bar{V} kT} \frac{\partial \mu_2(x, y, z, t)}{\partial z} \right]. \end{aligned}$$

Initial and boundary conditions for the above equations could be written as

$$\begin{aligned}
 & \left. \frac{\partial I(x, y, z, t)}{\partial x} \right|_{x=0} = 0, \left. \frac{\partial I(x, y, z, t)}{\partial x} \right|_{x=L_x} = 0, \left. \frac{\partial I(x, y, z, t)}{\partial y} \right|_{y=0} = 0, \\
 & \left. \frac{\partial I(x, y, z, t)}{\partial y} \right|_{y=L_y} = 0, \left. \frac{\partial I(x, y, z, t)}{\partial z} \right|_{z=0} = 0, \left. \frac{\partial I(x, y, z, t)}{\partial z} \right|_{z=L_z} = 0, \\
 & \left. \frac{\partial V(x, y, z, t)}{\partial x} \right|_{x=0} = 0, \left. \frac{\partial V(x, y, z, t)}{\partial x} \right|_{x=L_x} = 0, \left. \frac{\partial V(x, y, z, t)}{\partial y} \right|_{y=0} = 0, \quad (4) \\
 & \left. \frac{\partial V(x, y, z, t)}{\partial y} \right|_{y=L_y} = 0, \left. \frac{\partial V(x, y, z, t)}{\partial z} \right|_{z=0} = 0, \left. \frac{\partial V(x, y, z, t)}{\partial z} \right|_{z=L_z} = 0, I(x, y, z, 0) = \\
 & =f_i \quad (x, y, z), \quad V \quad (x, y, z, 0) = f_v \quad (x, y, z), \\
 & V(x_1 + V_n t, y_1 + V_n t, z_1 + V_n t, t) = V_\infty \left(1 + \frac{2 \ell \omega}{k T \sqrt{x_1^2 + y_1^2 + z_1^2}} \right).
 \end{aligned}$$

Here $I(x, y, z, t)$ is the spatio-temporal distribution of concentration of radiation interstitials; I^* is the equilibrium distribution of interstitials; $D_I(x, y, z, T)$, $D_V(x, y, z, T)$, $D_{IS}(x, y, z, T)$, $D_{VS}(x, y, z, T)$ are the coefficients of volumetric and surficial diffusions of interstitials and vacancies, respectively; terms $V^2(x, y, z, t)$ and $I^2(x, y, z, t)$ correspond to generation of divacancies and diinterstitials, respectively (see, for example, [25] and appropriate references in this book); $k_{I,V}(x, y, z, T)$, $k_{I,I}(x, y, z, T)$ and $k_{V,V}(x, y, z, T)$ are the parameters of recombination of point radiation defects and generation of their complexes; k is the Boltzmann constant; $\omega = a^3$, a is the interatomic distance; ℓ is the specific surface energy. To take into account porosity of the considered buffer layers we assume, that

the considered porous will be approximately cylindrical with average radius $r = \sqrt{x_1^2 + y_1^2}$ and length z_1 before annealing [22]. With time small pores decomposing on vacancies. The vacancies absorbing by larger pores [26]. During annealing the larger pores will be larger during absorption from smaller pores. The transformation of pores leads to more spherical form of pores [26]. Concentration of the considered vacancies could be estimated by the following sum (with account all pores)

$$V(x, y, z, t) = \sum_{i=0}^l \sum_{j=0}^m \sum_{k=0}^n V_p(x + i\alpha, y + j\beta, z + k\chi, t), \quad R = \sqrt{x^2 + y^2 + z^2},$$

where α , β and χ describes distances between pores in appropriate directions; parameters l , m and n describes quantities in the appropriate directions.

Distributions of concentrations in space and time of diinterstitials $\Phi_I(x, y, z, t)$ and divacancies $\Phi_V(x, y, z, t)$ could be obtained as solution of the next system of equations [24,25]

$$\begin{aligned}
 \frac{\partial \Phi_I(x, y, z, t)}{\partial t} &= \frac{\partial}{\partial x} \left[D_{\Phi_I}(x, y, z, T) \frac{\partial \Phi_I(x, y, z, t)}{\partial x} \right] + \frac{\partial}{\partial y} \left[D_{\Phi_I}(x, y, z, T) \frac{\partial \Phi_I(x, y, z, t)}{\partial y} \right] + \\
 &+ \frac{\partial}{\partial z} \left[D_{\Phi_I}(x, y, z, T) \frac{\partial \Phi_I(x, y, z, t)}{\partial z} \right] + \Omega \frac{\partial}{\partial x} \left[\frac{D_{\Phi_I S}}{kT} \nabla_S \mu_1(x, y, z, t) \int_0^{L_z} \Phi_I(x, y, W, t) dW \right] + \\
 &+ \Omega \frac{\partial}{\partial y} \left[\frac{D_{\Phi_I S}}{kT} \nabla_S \mu_1(x, y, z, t) \int_0^{L_z} \Phi_I(x, y, W, t) dW \right] + k_{I,I}(x, y, z, T) I^2(x, y, z, t) + \\
 &+ \frac{\partial}{\partial x} \left[\frac{D_{\Phi_I S}}{\bar{V} kT} \frac{\partial \mu_2(x, y, z, t)}{\partial x} \right] + \frac{\partial}{\partial y} \left[\frac{D_{\Phi_I S}}{\bar{V} kT} \frac{\partial \mu_2(x, y, z, t)}{\partial y} \right] + \frac{\partial}{\partial z} \left[\frac{D_{\Phi_I S}}{\bar{V} kT} \frac{\partial \mu_2(x, y, z, t)}{\partial z} \right] + \\
 &+ k_I(x, y, z, T) I(x, y, z, t) \tag{5}
 \end{aligned}$$

$$\begin{aligned}
 \frac{\partial \Phi_V(x, y, z, t)}{\partial t} &= \frac{\partial}{\partial x} \left[D_{\Phi_V}(x, y, z, T) \frac{\partial \Phi_V(x, y, z, t)}{\partial x} \right] + \frac{\partial}{\partial y} \left[D_{\Phi_V}(x, y, z, T) \frac{\partial \Phi_V(x, y, z, t)}{\partial y} \right] + \\
 &+ \frac{\partial}{\partial z} \left[D_{\Phi_V}(x, y, z, T) \frac{\partial \Phi_V(x, y, z, t)}{\partial z} \right] + \Omega \frac{\partial}{\partial x} \left[\frac{D_{\Phi_V S}}{kT} \nabla_S \mu_1(x, y, z, t) \int_0^{L_z} \Phi_V(x, y, W, t) dW \right] + \\
 &+ \Omega \frac{\partial}{\partial y} \left[\frac{D_{\Phi_V S}}{kT} \nabla_S \mu_1(x, y, z, t) \int_0^{L_z} \Phi_V(x, y, W, t) dW \right] + k_{V,V}(x, y, z, T) V^2(x, y, z, t) + \\
 &+ \frac{\partial}{\partial x} \left[\frac{D_{\Phi_V S}}{\bar{V} kT} \frac{\partial \mu_2(x, y, z, t)}{\partial x} \right] + \frac{\partial}{\partial y} \left[\frac{D_{\Phi_V S}}{\bar{V} kT} \frac{\partial \mu_2(x, y, z, t)}{\partial y} \right] + \frac{\partial}{\partial z} \left[\frac{D_{\Phi_V S}}{\bar{V} kT} \frac{\partial \mu_2(x, y, z, t)}{\partial z} \right] + \\
 &+ k_V(x, y, z, T) V(x, y, z, t).
 \end{aligned}$$

Initial and boundary conditions for the above equations could be written as

$$\begin{aligned}
 \left. \frac{\partial \Phi_I(x, y, z, t)}{\partial x} \right|_{x=0} &= 0, \quad \left. \frac{\partial \Phi_I(x, y, z, t)}{\partial x} \right|_{x=L_x} = 0, \quad \left. \frac{\partial \Phi_I(x, y, z, t)}{\partial y} \right|_{y=0} = 0, \\
 \left. \frac{\partial \Phi_I(x, y, z, t)}{\partial y} \right|_{y=L_y} &= 0, \quad \left. \frac{\partial \Phi_I(x, y, z, t)}{\partial z} \right|_{z=0} = 0, \quad \left. \frac{\partial \Phi_I(x, y, z, t)}{\partial z} \right|_{z=L_z} = 0, \\
 \left. \frac{\partial \Phi_V(x, y, z, t)}{\partial x} \right|_{x=0} &= 0, \quad \left. \frac{\partial \Phi_V(x, y, z, t)}{\partial x} \right|_{x=L_x} = 0, \quad \left. \frac{\partial \Phi_V(x, y, z, t)}{\partial y} \right|_{y=0} = 0, \tag{6} \\
 \left. \frac{\partial \Phi_V(x, y, z, t)}{\partial y} \right|_{y=L_y} &= 0, \quad \left. \frac{\partial \Phi_V(x, y, z, t)}{\partial z} \right|_{z=0} = 0, \quad \left. \frac{\partial \Phi_V(x, y, z, t)}{\partial z} \right|_{z=L_z} = 0,
 \end{aligned}$$

$$\Phi_I(x, y, z, 0) = f_{\Phi_I}(x, y, z), \quad \Phi_V(x, y, z, 0) = f_{\Phi_V}(x, y, z).$$

Here $D_{\Phi_I}(x, y, z, T)$, $D_{\Phi_V}(x, y, z, T)$, $D_{\Phi_I S}(x, y, z, T)$ and $D_{\Phi_V S}(x, y, z, T)$ are the coefficients of volumetric and surficial diffusions of complexes of radiation defects; $k_I(x, y, z, T)$ and $k_V(x, y, z, T)$ are the pa-

parameters of decay of complexes of radiation defects.

Chemical potential μ_1 , which were presented in Eqs. (1), (3) and (5), could be obtained by the relation, which is presented bellow [19]

$$\mu_1 = E(z)\Omega\sigma_{ij}[u_{ij}(x,y,z,t)+u_{ji}(x,y,z,t)]/2. \quad (7)$$

In the above relation $E(z)$ describes the Young modulus, value σ_{ij} describes the tensor of stress;

value $u_{ij} = \frac{1}{2} \left(\frac{\partial u_i}{\partial x_j} + \frac{\partial u_j}{\partial x_i} \right)$ is the deformation tensor; u_i, u_j are the components $u_x(x,y,z,t),$

$u_y(x,y,z,t)$ and $u_z(x,y,z,t)$ of the displacement vector $\vec{u}(x, y, z, t)$; x_i, x_j are the coordinate $x, y, z.$ The Eq. (3) could be written as

$$\begin{aligned} \mu(x, y, z, t) = & \left[\frac{\partial u_i(x, y, z, t)}{\partial x_j} + \frac{\partial u_j(x, y, z, t)}{\partial x_i} \right] \left\{ \frac{1}{2} \left[\frac{\partial u_i(x, y, z, t)}{\partial x_j} + \frac{\partial u_j(x, y, z, t)}{\partial x_i} \right] - \right. \\ & \left. - \varepsilon_0 \delta_{ij} + \frac{\sigma(z)\delta_{ij}}{1-2\sigma(z)} \left[\frac{\partial u_k(x, y, z, t)}{\partial x_k} - 3\varepsilon_0 \right] - K(z)\beta(z)[T(x, y, z, t) - T_0] \delta_{ij} \right\} \frac{\Omega}{2} E(z). \end{aligned}$$

Here value σ describes the coefficient of Poisson; $\varepsilon_0 = (a_s - a_{EL})/a_{EL}$ is the mismatch parameter; a_s, a_{EL} are lattice distances of the substrate and the epitaxial layer; K is the modulus of uniform compression; β is the coefficient of thermal expansion; T_r is the equilibrium temperature, which coincide (for our case) with room temperature. Components of displacement vector could be obtained by solution of the following equations [20]

$$\begin{aligned} \rho(z) \frac{\partial^2 u_x(x, y, z, t)}{\partial t^2} &= \frac{\partial \sigma_{xx}(x, y, z, t)}{\partial x} + \frac{\partial \sigma_{xy}(x, y, z, t)}{\partial y} + \frac{\partial \sigma_{xz}(x, y, z, t)}{\partial z} \\ \rho(z) \frac{\partial^2 u_y(x, y, z, t)}{\partial t^2} &= \frac{\partial \sigma_{yx}(x, y, z, t)}{\partial x} + \frac{\partial \sigma_{yy}(x, y, z, t)}{\partial y} + \frac{\partial \sigma_{yz}(x, y, z, t)}{\partial z} \\ \rho(z) \frac{\partial^2 u_z(x, y, z, t)}{\partial t^2} &= \frac{\partial \sigma_{zx}(x, y, z, t)}{\partial x} + \frac{\partial \sigma_{zy}(x, y, z, t)}{\partial y} + \frac{\partial \sigma_{zz}(x, y, z, t)}{\partial z}, \end{aligned}$$

where

$$\begin{aligned} \sigma_{ij} = & \frac{E(z)}{2[1+\sigma(z)]} \left[\frac{\partial u_i(x, y, z, t)}{\partial x_j} + \frac{\partial u_j(x, y, z, t)}{\partial x_i} - \frac{\delta_{ij}}{3} \frac{\partial u_k(x, y, z, t)}{\partial x_k} \right] + K(z)\delta_{ij} \times \\ & \times \frac{\partial u_k(x, y, z, t)}{\partial x_k} - \beta(z)K(z)[T(x, y, z, t) - T_r], \rho(z) \text{ is the density of materials of hete} \end{aligned}$$

rostructure, δ_{ij} Is the Kronecker symbol. Accounting of the relation for σ_{ij} into the last system of equation could be written in the following form

$$\begin{aligned}
 \rho(z) \frac{\partial^2 u_x(x, y, z, t)}{\partial t^2} &= \left\{ K(z) + \frac{5E(z)}{6[1+\sigma(z)]} \right\} \frac{\partial^2 u_x(x, y, z, t)}{\partial x^2} + \left\{ K(z) - \frac{E(z)}{3[1+\sigma(z)]} \right\} \times \\
 &\times \frac{\partial^2 u_y(x, y, z, t)}{\partial x \partial y} + \frac{E(z)}{2[1+\sigma(z)]} \left[\frac{\partial^2 u_y(x, y, z, t)}{\partial y^2} + \frac{\partial^2 u_z(x, y, z, t)}{\partial z^2} \right] + \left[K(z) + \frac{E(z)}{3[1+\sigma(z)]} \right] \times \\
 &\times \frac{\partial^2 u_z(x, y, z, t)}{\partial x \partial z} - K(z) \beta(z) \frac{\partial T(x, y, z, t)}{\partial x} \\
 \rho(z) \frac{\partial^2 u_y(x, y, z, t)}{\partial t^2} &= \frac{E(z)}{2[1+\sigma(z)]} \left[\frac{\partial^2 u_y(x, y, z, t)}{\partial x^2} + \frac{\partial^2 u_x(x, y, z, t)}{\partial x \partial y} \right] - \frac{\partial T(x, y, z, t)}{\partial y} \times \\
 &\times K(z) \beta(z) + \frac{\partial}{\partial z} \left\{ \frac{E(z)}{2[1+\sigma(z)]} \left[\frac{\partial u_y(x, y, z, t)}{\partial z} + \frac{\partial u_z(x, y, z, t)}{\partial y} \right] \right\} + \frac{\partial^2 u_y(x, y, z, t)}{\partial y^2} \times \quad (8) \\
 &\times \left\{ \frac{5E(z)}{12[1+\sigma(z)]} + K(z) \right\} + \left\{ K(z) - \frac{E(z)}{6[1+\sigma(z)]} \right\} \frac{\partial^2 u_y(x, y, z, t)}{\partial y \partial z} + K(z) \frac{\partial^2 u_y(x, y, z, t)}{\partial x \partial y} \\
 \rho(z) \frac{\partial^2 u_z(x, y, z, t)}{\partial t^2} &= \frac{E(z)}{2[1+\sigma(z)]} \left[\frac{\partial^2 u_z(x, y, z, t)}{\partial x^2} + \frac{\partial^2 u_z(x, y, z, t)}{\partial y^2} + \frac{\partial^2 u_x(x, y, z, t)}{\partial x \partial z} \right. \\
 &+ \left. \frac{\partial^2 u_y(x, y, z, t)}{\partial y \partial z} \right] + \frac{\partial}{\partial z} \left\{ K(z) \left[\frac{\partial u_x(x, y, z, t)}{\partial x} + \frac{\partial u_y(x, y, z, t)}{\partial y} + \frac{\partial u_x(x, y, z, t)}{\partial z} \right] \right\} + \\
 &+ \frac{1}{6} \frac{\partial}{\partial z} \left\{ \frac{E(z)}{1+\sigma(z)} \left[6 \frac{\partial u_z(x, y, z, t)}{\partial z} - \frac{\partial u_x(x, y, z, t)}{\partial x} - \frac{\partial u_y(x, y, z, t)}{\partial y} - \frac{\partial u_z(x, y, z, t)}{\partial z} \right] \right\} - \\
 &- K(z) \beta(z) \frac{\partial T(x, y, z, t)}{\partial z}.
 \end{aligned}$$

Conditions for the system of Eq. (8) could be written in the form

$$\begin{aligned}
 \frac{\partial \bar{u}(0, y, z, t)}{\partial x} &= 0; \quad \frac{\partial \bar{u}(L_x, y, z, t)}{\partial x} = 0; \quad \frac{\partial \bar{u}(x, 0, z, t)}{\partial y} = 0; \quad \frac{\partial \bar{u}(x, L_y, z, t)}{\partial y} = 0; \\
 \frac{\partial \bar{u}(x, y, 0, t)}{\partial z} &= 0; \quad \frac{\partial \bar{u}(x, y, L_z, t)}{\partial z} = 0; \quad \bar{u}(x, y, z, 0) = \bar{u}_0; \quad \bar{u}(x, y, z, \infty) = \bar{u}_0.
 \end{aligned}$$

All considered equations (equations (1), (3), (5) and (8)) were solved by the method of averaging of function corrections [27]. In the framework of the paper we determine concentration of dopant, concentrations of radiation defects and components of displacement vector by using the second-order approximation in the framework of the method of averaging of function corrections. This approximation is usually enough good approximation to make qualitative analysis and to obtain some quantitative results. All obtained results have been checked by comparison with results of numerical simulations.

3. DISCUSSION

In this section we analyzed dynamics of redistributions of dopant and radiation defects during annealing and under influence of mismatch-induced stress and modification of porosity. Typical distributions of concentrations of dopant in heterostructures are presented on Figs. 2 and 3 for diffusion and ion types of doping, respectively. These distributions have been calculated for the case, when value of dopant diffusion coefficient in doped area is larger, than in nearest areas. The figures show, that inhomogeneity of heterostructure gives us possibility to increase compactness of concentrations of dopants and at the same time to increase homogeneity of dopant distribution in doped part of epitaxial layer. Changing of distribution of concentration of dopant in heterostructure in comparison with homogenous sample was obtained due to lower value of dopant diffusion coefficient in substrate in comparison with epitaxial layer.

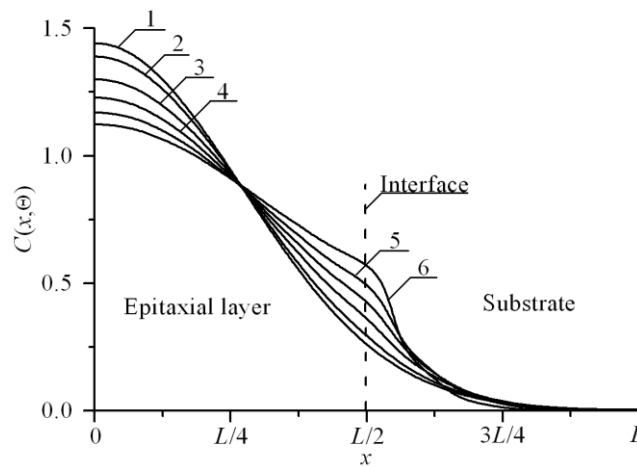


Fig. 2. Distributions of concentration of infused dopant in heterostructure from Fig. 1 in direction, which is perpendicular to interface between epitaxial layer substrate. Increasing of number of curve corresponds to increasing of difference between values of dopant diffusion coefficient in layers of heterostructure under condition, when value of dopant diffusion coefficient in epitaxial layer is larger, than value of dopant diffusion coefficient in substrate

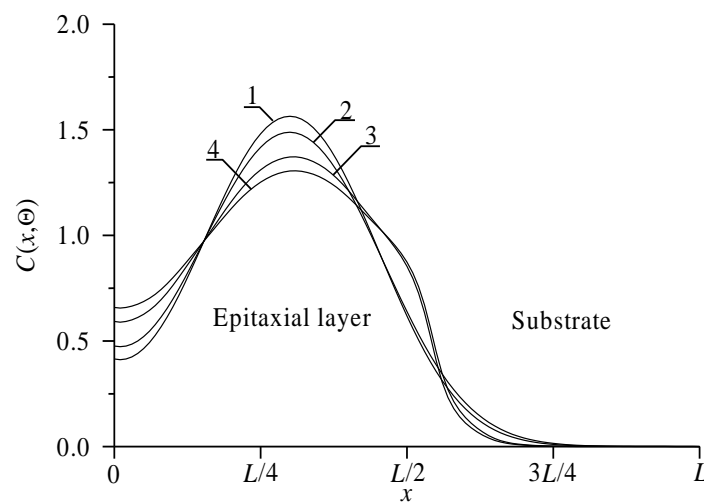


Fig. 3. Distributions of concentration of implanted dopant in heterostructure from Fig. 1 in direction, which is perpendicular to interface between epitaxial layer substrate. Curves 1 and 3 corresponds to annealing

time $\Theta = 0.0048(L_x^2+L_y^2+L_z^2)/D_0$. Curves 2 and 4 corresponds to annealing time $\Theta = 0.0057(L_x^2+L_y^2+L_z^2)/D_0$.

Curves 1 and 2 corresponds to homogenous sample. Curves 3 and 4 corresponds to heterostructure under condition, when value of dopant diffusion coefficient in epitaxial layer is larger, than value of dopant diffusion coefficient in substrate

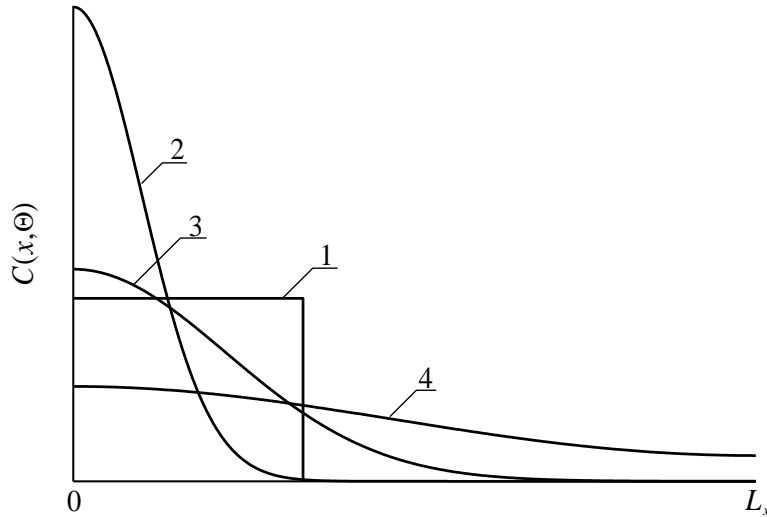


Fig. 4. Spatial distributions of dopant in heterostructure after dopant infusion. Curve 1 is idealized distribution of dopant. Curves 2-4 are real distributions of dopant for different values of annealing time. Increasing of number of curve corresponds to increasing of annealing time

At the same time using the approach of manufacturing of field-effect transistor leads to optimization of annealing of dopant and/or radiation defects. Reason of this optimization is following. If annealing time is small, the dopant did not achieve any interfaces between materials of heterostructure. In this situation no modifications of distribution of dopant's concentration were obtained. If annealing time is large, distribution of concentration of dopant is too homogenous. Now let us to optimize the annealing time by using the recently introduces approach [28-36]. In the framework of the criterion one shall to approximate real distribution of dopant's concentration by the following step-wise function (see Figs. 4 and 5). Next we determine optimal values of annealing time by minimization of the following mean-squared error

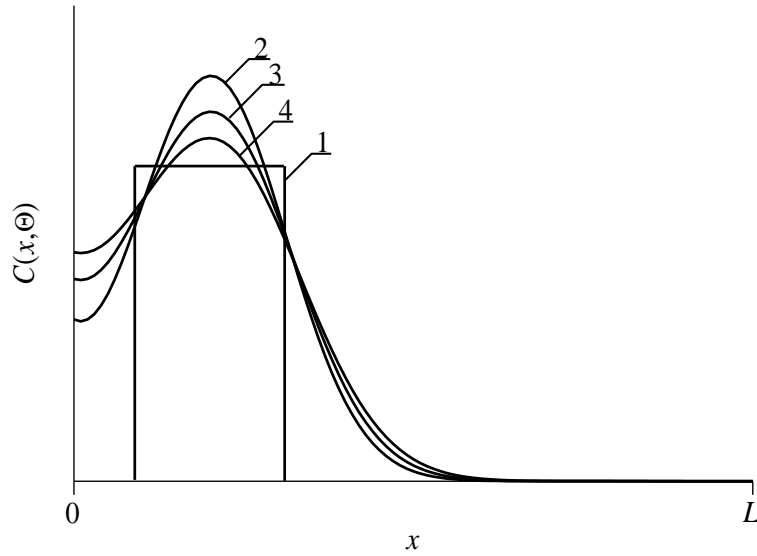


Fig. 5. Spatial distributions of dopant in heterostructure after ion implantation. Curve 1 is idealized distribution of dopant. Curves 2-4 are real distributions of dopant for different values of annealing time. Increasing of number of curve corresponds to increasing of annealing time

$$U = \frac{1}{L_x L_y L_z} \int_0^{L_x} \int_0^{L_y} \int_0^{L_z} [C(x, y, z, \Theta) - \psi(x, y, z)] dz dy dx, \quad (11)$$

where $\psi(x,y,z)$ is the step-wise approximation function. Dependences of optimal values of annealing time on parameters are presented on Figs. 6 and 7 for diffusion and ion types of doping, respectively. It should be noted, that it is necessary to anneal radiation defects after ion implantation. One could find spreading of concentration of distribution of dopant during this annealing. In the ideal case distribution of dopant achieves appropriate interfaces between materials of heterostructure during annealing of radiation defects. If dopant did not achieves any interfaces during annealing of radiation defects, it is practicably to additionally anneal the dopant. In this situation optimal value of additional annealing time of implanted dopant is smaller, than annealing time of infused dopant. Increasing of the optimal values of annealing time were obtain by increasing of value of dopant diffusion coefficient with changing of the considered parameters.

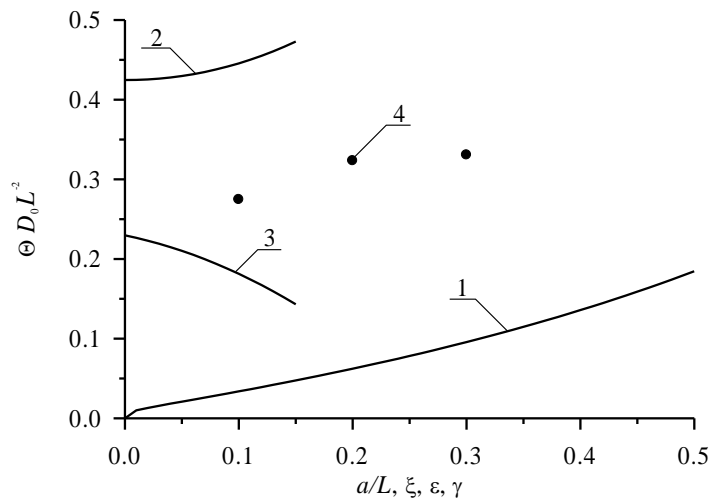


Fig. 6. Dependences of dimensionless optimal annealing time for doping by diffusion, which have been obtained by minimization of mean-squared error, on several parameters.

Curve 1 is the dependence of dimensionless optimal annealing time on the relation a/L and $\xi = \gamma = 0$ for equal to each other values of dopant diffusion coefficient in all parts of heterostructure. Curve 2 is the dependence of dimensionless optimal annealing time on value of parameter ε for $a/L=1/2$ and $\xi = \gamma = 0$. Curve 3 is the dependence of dimensionless optimal annealing time on value of parameter ξ for $a/L=1/2$ and $\varepsilon = \gamma = 0$. Curve 4 is the dependence of dimensionless optimal annealing time on value of parameter γ for $a/L=1/2$ and $\varepsilon = \xi = 0$

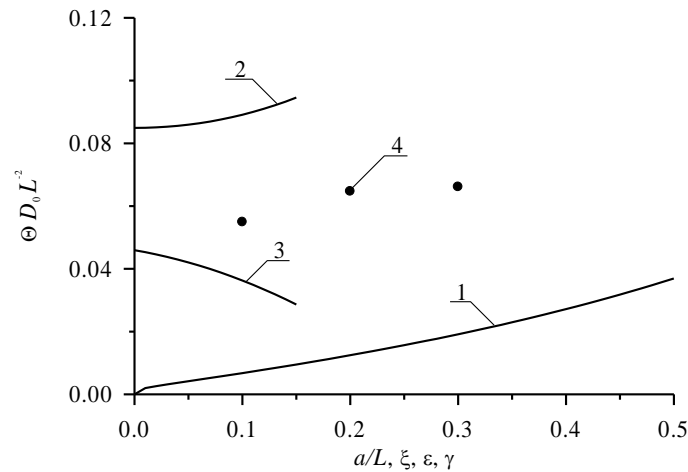


Fig. 7. Dependences of dimensionless optimal annealing time for doping by ion implantation, which have been obtained by minimization of mean-squared error, on several parameters.

Curve 1 is the dependence of dimensionless optimal annealing time on the relation a/L and $\xi = \gamma = 0$ for equal to each other values of dopant diffusion coefficient in all parts of heterostructure. Curve 2 is the dependence of dimensionless optimal annealing time on value of parameter ε for $a/L=1/2$ and $\xi = \gamma = 0$. Curve 3 is the dependence of dimensionless optimal annealing time on value of parameter ξ for $a/L=1/2$ and $\varepsilon = \gamma = 0$. Curve 4 is the dependence of dimensionless optimal annealing time on value of parameter γ for $a/L=1/2$ and $\varepsilon = \xi = 0$

Next we analyzed influence of relaxation of mismatch-induced stress on distribution of dopant in doped areas of heterostructure. Under following condition $\varepsilon_0 < 0$ one can find compression of distribution of concentration of dopant near interface between materials of heterostructure. Contrary (at $\varepsilon_0 > 0$) one can find spreading of distribution of concentration of dopant in this area. This changing of distribution of concentration of dopant could be at least partially compensated by using laser annealing [36]. The considered annealing leads to acceleration dopant diffusion and another processes in processed area due to inhomogeneity of temperature distribution and law of Arrhenius. Accounting relaxation of mismatch-induced stress in heterostructure could leads to changing of optimal values of annealing time. It should be noted, that modification of porosity leads to decreasing of value of mismatch-induced stress. On the one hand mismatch-induced stress could be used to increase density of elements of integrated circuits. On the other hand could leads to generation dislocations of the discrepancy. Figs. 8 and 9 show distributions of vacancies concentration in the porous materials and displacement vector's component. The component is perpendicular to interface, which is presents between layers of the considered heterostructure. Increasing of quantity of vacancies leads to decreasing of component u_z of displacement vector due to decreasing of density of materials of heterostructure. At the same time one can find

decreasing of quantity of vacancies due to presents of mismatch-induced stress.

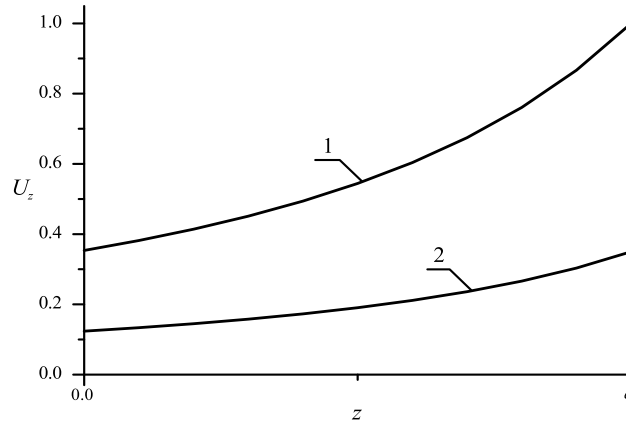


Fig. 8. Normalized dependences of component u_z of displacement vector on coordinate z for nonporous (curve 1) and porous (curve 2) epitaxial layers

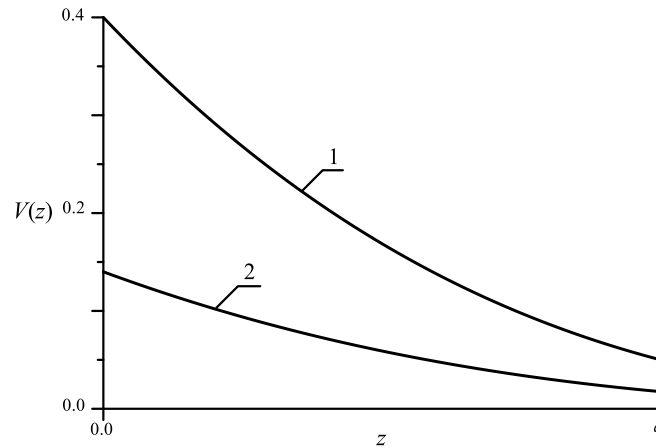


Fig. 9. Normalized dependences of vacancy concentrations on coordinate z in unstressed (curve 1) and stressed (curve 2) epitaxial layers

4. CONCLUSION

In this paper we model redistribution of infused and implanted dopants with account relaxation mismatch-induced stress during manufacturing field-effect heterotransistors in the framework of the CMOS operational transresistance amplifier based square wave generator. We formulate recommendations for optimization of annealing to decrease dimensions of transistors and to increase their density. We formulate recommendations to decrease mismatch-induced stress. Analytical approach to model diffusion and ion types of doping with account concurrent changing of parameters in space and time has been introduced. At the same time the approach gives us possibility to take into account nonlinearity of considered processes.

5. FUTURE WORK

Results of this paper could be used to optimize manufacturing of integrated circuits to increase density of elements of integrated circuits and to decrease their dimensions.

REFERENCES

- [1] V.I. Lachin, N.S. Savelov. Electronics (Rostov-on-Don: Phoenix, 2001).
- [2] A. Polishcuk. Modern Electronics. Issue 12. P. 8-11 (2004).
- [3] G. Volovich. Modern Electronics. Issue 2. P. 10-17 (2006).
- [4] A. Kerentsev, V. Lanin. Power Electronics. Issue 1. P. 34 (2008).
- [5] A.O. Ageev, A.E. Belyaev, N.S. Boltovets, V.N. Ivanov, R.V. Konakova, Ya.Ya. Kudrik, P.M. Litvin, V.V. Milenin, A.V. Sachenko. Semiconductors. Vol. 43 (7). P. 897-903 (2009).
- [6] Jung-Hui Tsai, Shao-Yen Chiu, Wen-Shiung Lour. Der-Feng Guo. Semiconductors. Vol. 43 (7). C. 971-974 (2009).
- [7] O.V. Alexandrov, A.O. Zakhar'in, N.A. Sobolev, E.I. Shek, M.M. Ma-koviychuk, E.O. Parshin. Semiconductors. Vol. 32 (9). P. 1029-1032 (1998).
- [8] I.B. Ermolovich, V.V. Milenin, R.A. Red'ko, S.M. Red'ko. Semiconductors. Vol. 43 (8). P. 1016-1020 (2009).
- [9] P. Sinsermsuksakul, K. Hartman, S.B. Kim, J. Heo, L. Sun, H.H. Park, R. Chakraborty, T. Buonassisi, R.G. Gordon. Appl. Phys. Lett. Vol. 102 (5). P. 053901-053905 (2013).
- [10] J.G. Reynolds, C.L. Reynolds, Jr.A. Mohanta, J.F. Muth, J.E. Rowe, H.O. Everitt, D.E. Aspnes. Appl. Phys. Lett. Vol. 102 (15). P. 152114-152118 (2013).
- [11] N.I. Volokobinskaya, I.N. Komarov, T.V. Matyukhina, V.I. Reshetnikov, A.A. Rush, I.V. Falina, A.S. Yastrebov. Semiconductors. Vol. 35 (8). P. 1013-1017 (2001).
- [12] E.L. Pankratov, E.A. Bulaeva. Reviews in Theoretical Science. Vol. 1 (1). P. 58-82 (2013).
- [13] S.A. Kukushkin, A.V. Osipov, A.I. Romanychev. Physics of the Solid State. Vol. 58 (7). P. 1448-1452 (2016).
- [14] E.M. Trukhanov, A.V. Kolesnikov, I.D. Loshkarev. Russian Microelectronics. Vol. 44 (8). P. 552-558 (2015).
- [15] E.L. Pankratov, E.A. Bulaeva. Reviews in Theoretical Science. Vol. 3 (4). P. 365-398 (2015).
- [16] K.K. Ong, K.L. Pey, P.S. Lee, A.T.S. Wee, X.C. Wang, Y.F. Chong, Appl. Phys. Lett. Vol. 89 (17). P. 172111-172114 (2006).
- [17] Yu.V. Bykov, A.G. Yermeev, N.A. Zharova, I.V. Plotnikov, K.I. Rybakov, M.N. Drozdov, Yu.N. Drozdov, V.D. Skupov. Radiophysics and Quantum Electronics. Vol. 43 (3). P. 836-843 (2003).
- [18] Gh. Singh, Md.H. Pasha, M. Shashidhar, Z. Tabassum. International journal of innovative research in electronics and communications. Vol. 6 (1). P. 1-6 (2019).
- [19] Y.W. Zhang, A.F. Bower. Journal of the Mechanics and Physics of Solids. Vol. 47 (11). P. 2273-2297 (1999).
- [20] L.D. Landau, E.M. Lifshits. Theoretical physics. 7 (Theory of elasticity) (Physmatlit, Moscow, 2001).
- [21] M. Kitayama, T. Narushima, W.C. Carter, R.M. Cannon, A.M. Glaeser. J. Am. Ceram. Soc. Vol. 83. P. 2561 (2000); M. Kitayama, T. Narushima, A.M. Glaeser. J. Am. Ceram. Soc. Vol. 83. P. 2572 (2000).
- [22] P.G. Cheremskoy, V.V. Slesov, V.I. Betekhtin. Pore in solid bodies (Energoatomizdat, Moscow, 1990).
- [23] Z.Yu. Gotra. Technology of microelectronic devices (Radio and communication, Moscow, 1991).
- [24] P.M. Fahey, P.B. Griffin, J.D. Plummer. Rev. Mod. Phys. Vol. 61 (2). P. 289-388 (1989).
- [25] V.L. Vinetskiy, G.A. Kholodar', Radiative physics of semiconductors. ("Naukova Dumka", Kiev, 1979).
- [26] M.G. Mynbaeva, E.N. Mokhov, A.A. Lavrent'ev, K.D. Mynbaev, Techn. Phys. Lett. Vol. 34 (17). P. 13 (2008).
- [27] Yu.D. Sokolov. Applied Mechanics. Vol.1 (1). P. 23-35 (1955).
- [28] E.L. Pankratov. Russian Microelectronics. Vol. 36 (1). P. 33-39 (2007).
- [29] E.L. Pankratov. Int. J. Nanoscience. Vol. 7 (4-5). P. 187-197 (2008).
- [30] E.L. Pankratov, E.A. Bulaeva. Reviews in Theoretical Science. Vol. 1 (1). P. 58-82 (2013).
- [31] E.L. Pankratov, E.A. Bulaeva. Int. J. Micro-Nano Scale Transp. Vol. 3 (3). P. 119-130 (2012).
- [32] E.L. Pankratov, E.A. Bulaeva. International Journal of Modern Physics B. Vol. 29 (5). P. 1550023-1-1550023-12 (2015).
- [33] E.L. Pankratov. J. Comp. Theor. Nanoscience. Vol. 14 (10). P. 4885-4899 (2017).
- [34] E.L. Pankratov, E.A. Bulaeva. Materials science in semiconductor processing. Vol. 34. P. 260-268 (2015).

- [35] E.L. Pankratov, E.A. Bulaeva. *Int. J. Micro-Nano Scale Transp.* Vol. 4 (1). P. 17-31 (2014).
- [36] E.L. Pankratov, E.A. Bulaeva. *Multidiscipline modeling in materials and structures.* Vol. 12 (4). P. 578-604 (2016).